Electronic Supplementary Material (ESI) for Physical Chemistry Chemical Physics.

Electronic Supplementary Information for Hydrolysis of Cephalexin and Meropenem by New Delhi Metallo β–Lactamase: Substrate Protonation Mechanism is Drug Dependent

Chandan Kumar Das and Nisanth N. Nair*

Department of Chemistry, Indian Institute Of Technology Kanpur, Kanpur, 208016, India

E-mail: nnair@iitk.ac.in

S1 Active Site Structure

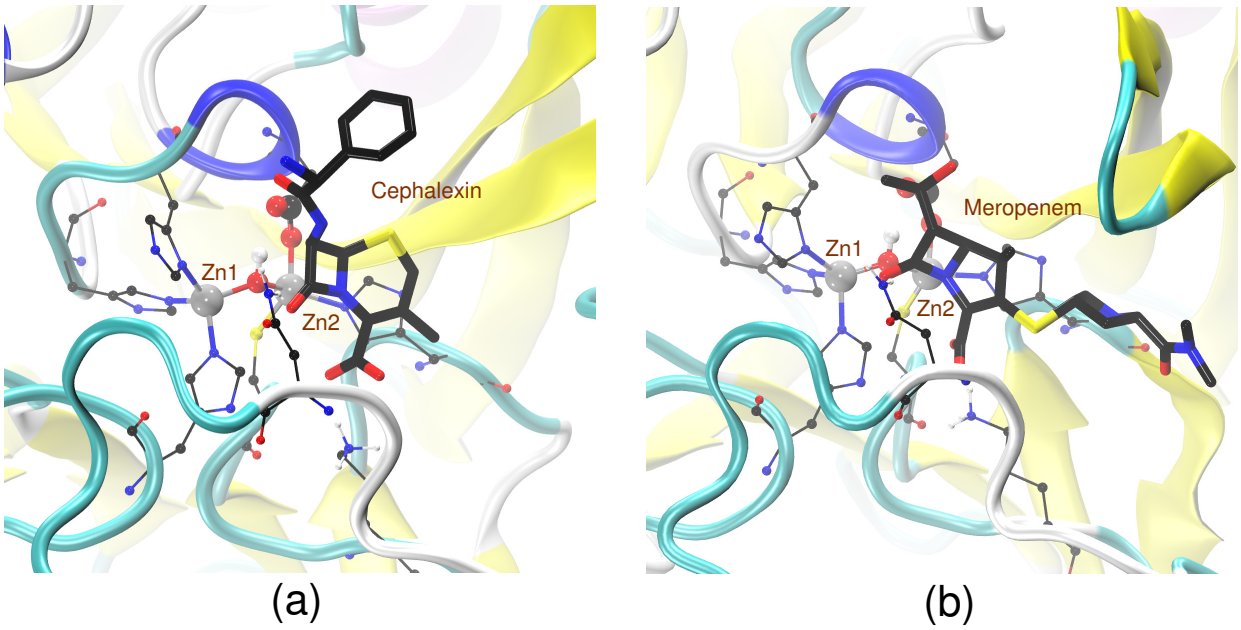

Figure S1: Equilibrated active site structure of NDM-1:cephalexin Michaelis complex (**ES**) (a) and NDM-1:meropenem Michaelis complex (**ES**) (b).

S2 Active Site Structure with QM/MM partition

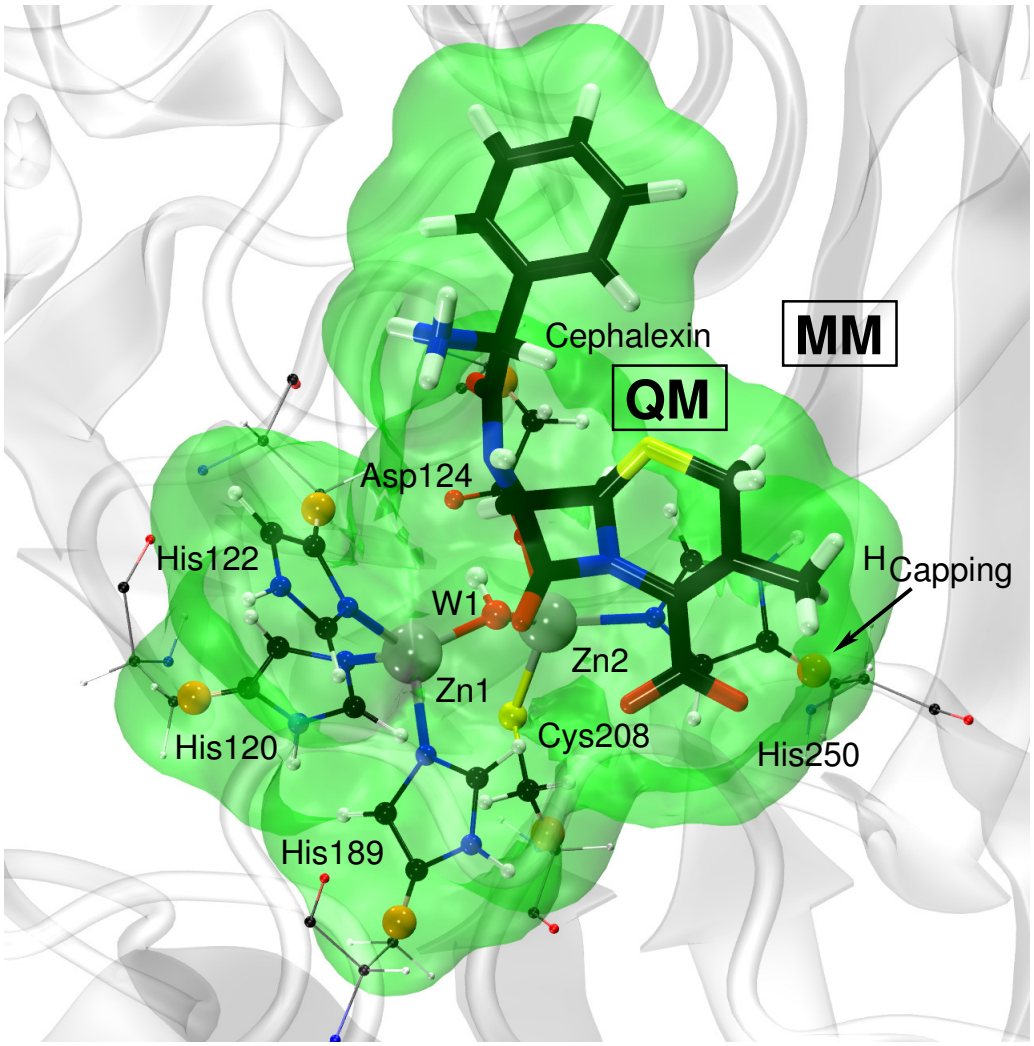

Figure S2: Active site of cephalexin bound NDM-1 is shown here. The highlighted atoms together with the drug molecule were treated by QM and the rest of the system were treated by MM. Capping H atoms are shown in orange color. Electron density of the QM part computed for the given snapshot is shown in green color. The QM/MM regions are treated by the same way for simulating meropenem bound NDM-1.

S3 RMSD Curves from MM MD Simulation of Michaelis Complexes (ES)

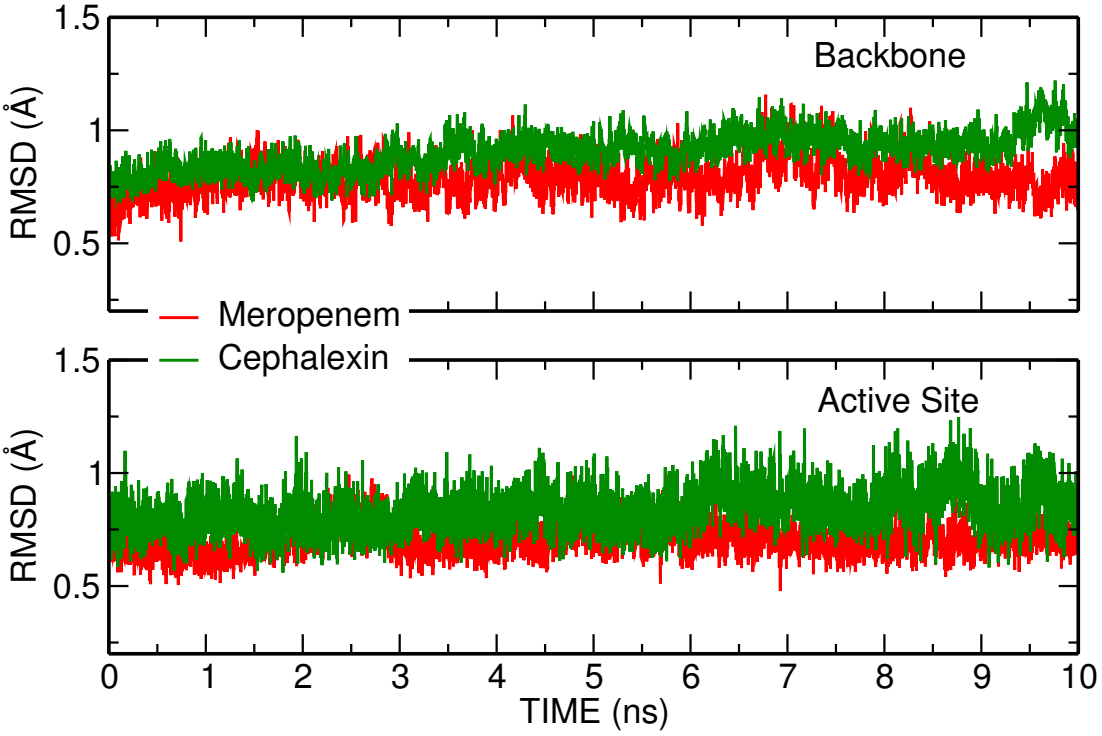

Figure S3: RMSD of the heavy atoms part of the protein backbone (top) and the active site (which includes His120, His122, Asp124, His189, Cys208, His250, Zn1, Zn2 and W1) for NDM-1:cephalexin (green) and NDM-1:meropenem (red) **ES** structure with respect to X-ray structures (PDB IDs: 4RL2[1] and 4EYL,[2] respectively).

S4 Average Distances in the Equilibrated Active Site of Michaelis Complex (ES)

Table S1: Crucial distances (in Å) computed during MM MD simulation for the **ES** structure.

Atoms	NDM-1:cephalexin	NDM-1:meropenem
Zn1...Zn2	3.35±0.09	3.32±0.09
Zn1...O_1	3.65±0.31	4.21±0.33
Zn2...O_9	4.42±0.29	5.13±0.28
C_8...Lys211:N_ζ	3.38±0.11	3.33±0.13
O_1...Asn220:$H_{\delta 1}$	2.79±0.79	2.14±0.40
C_2...O_{W1}	3.02±0.16	3.57±0.24
H_{W1}...Asp124:$O_{\delta 1}$	1.67±0.09	1.72±0.12

Table S2: Crucial distances (in Å) computed during QM/MM MD simulation for the **ES** structure.

Atoms	NDM-1:cephalexin	NDM-1:meropenem
Zn1...Zn2	3.49±0.11	3.44±0.15
Zn1...O_1	4.13±0.32	3.85±0.27
Zn2...O_9	4.14±0.41	3.67±0.61
C_8...Lys211:N_ζ	3.19±0.12	3.42±0.19
O_1...Asn220:$H_{\delta 1}$	1.94±0.19	2.04±0.25
C_2...O_{W1}	3.40±0.23	3.21±0.23
H_{W1}...Asp124:$O_{\delta 1}$	1.78±0.14	1.78±0.16

S5 Mechanistic Pathways

Table S3: Pathways studied here in the NDM-1 catalyzed β–lactam hydrolysis with computed free energy barriers (kcal mol^{-1}) for various elementary steps.

Reactions	Cephalexin	Meropenem
Path 1 : ES → EI1 → EI2 → EI3 → EP		
ES → EI1	20±2	20±2
EI1 → ES	32±3	34±3
EI1 → EI2†	25±1	24±1
EI2 → EI1	11±3	11±3‡
EI2 → EI3	9±3	8±3
EI3 → EP	10±3	13±3
Path 2 : ES → EI1 → EI4		
EI1 → EI4	36±3	–
Path 3 : ES → EI1 → EI2′ → EI3′ → EI4′ → EP1′ → EP2′		
EI1 → EI2′	13±3	–
EI2′ → EI1	>30±3	–
EI2′ → EI3′†	18±1	–
EI3′ → EI2′	8±3	–
EI3′ → EI4′†	13±1	–
EI4′ → EP1′	15±3	–
EP1′ → EP2′	6±3	–
Path 4 : ES → EI1 → EI2 → EI3 → EI6′		
EI3 → EI6′	>30±3	–
Path 5 : ES → EI1 → EI5		
EI1 → EI5	>30±3	–

† Free energy barrier for **EI1** $\rightarrow$ **EI2** (**Path 1**), **EI2′** $\rightarrow$ **EI3′** (**Path 3**) and **EI3′** $\rightarrow$ **EI4′** (**Path 3**) were computed using well–sliced metadynamics simulation. The free energy barrier for **EI1** $\rightarrow$ **EI2** of meropenem is directly taken from our earlier work.[3]

‡ The free energy barrier for **EI2** $\rightarrow$ **EI1** (**Path 1**) for meropenem was assumed to be same as that of cephalexin.

S6 Structures of Various Reaction Intermediates of Meropenem Hydrolysis

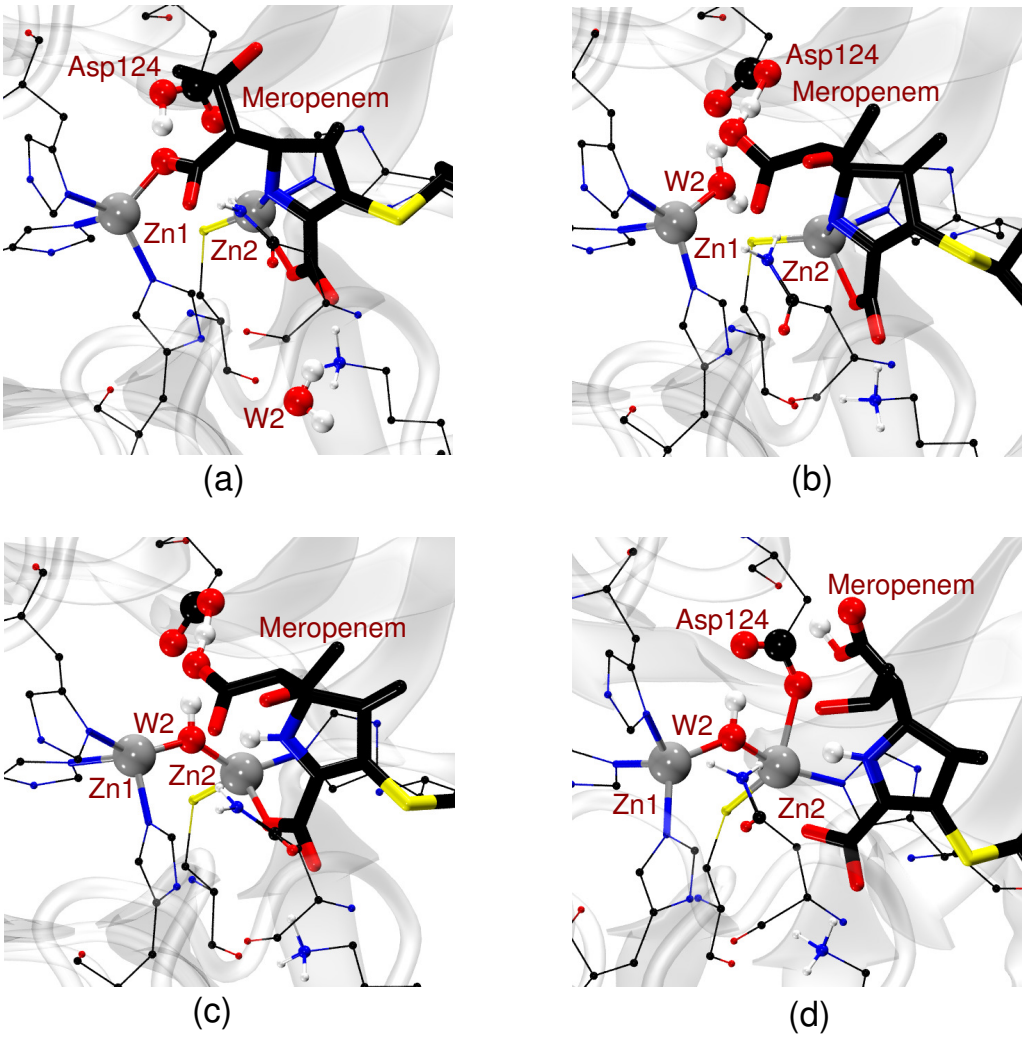

Figure S4: Equilibrated structures of NDM-1:meropenem complexes corresponding to **EI1** (a), **EI2** (b), **EI3** (c) and **EP** (d).

S7 W2 Entry to Active site

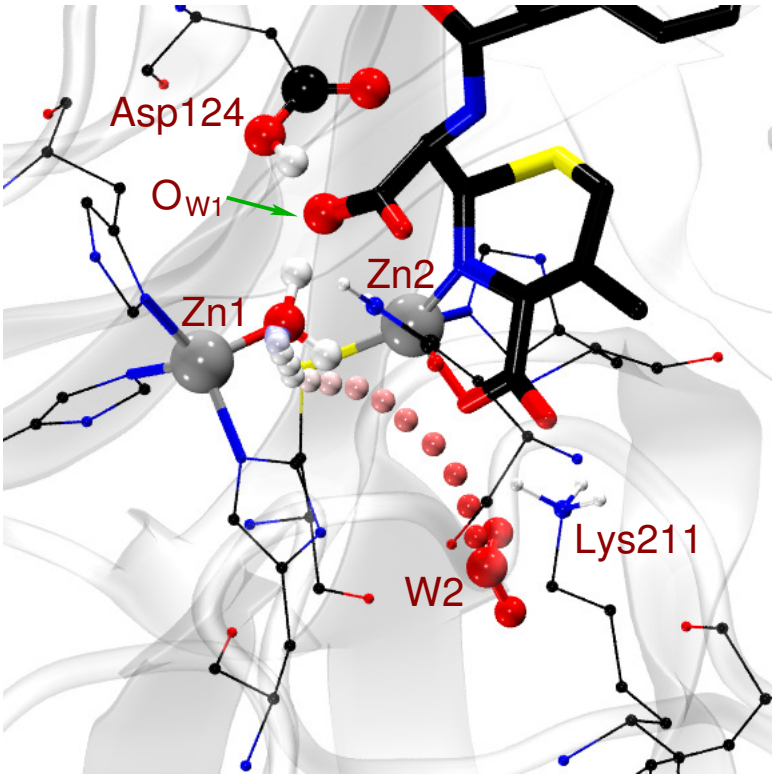

Figure S5: Structure **EI2** together with path (small glossy spheres with colors varying from red to white with the progress of the reaction) followed by W2 while diffusing towards the active site during the reaction of **EI1** $\rightarrow$ **EI2**.

S8 Details of Metadynamics Setup

We have employed the extended Lagrangian metadynamics technique. The biasing potentials were spherical Gaussian functions with their heights fixed to 1.6 kcal mol^{-1} and the width of the Gaussian function was fixed to 0.05. An adaptive metadynamics time step is used where the Gaussian bias is updated only when the displacement of the CVs in the CV space is greater than 0.075 (which is 1.5 times the Gaussian width parameter). The harmonic coupling constant connecting collective variables (CVs) and collective coordinates (CCs) was taken as 2.0 a.u. CV temperature was maintained within the window of 300±200 K using velocity scaling.

Definition of CVs:

We have mostly used coordination number type CVs. Coordination number of A atom with a group of B atoms, C[A...B], is defined by

$$C[\mathrm{A}-\mathrm{B}] = \sum_{J \in \mathrm{B}} \frac{1-\left(\frac{d_{\mathrm{A}J}}{d^0_{\mathrm{AB}}}\right)^p}{1-\left(\frac{d_{\mathrm{A}J}}{d^0_{\mathrm{AB}}}\right)^{p+q}} \tag{1}$$

where $d_{\mathrm{A}J}$ is the distance between atoms A and J, while d^0_{AB} is a cutoff distance parameter. Here p and q are even integer parameters.

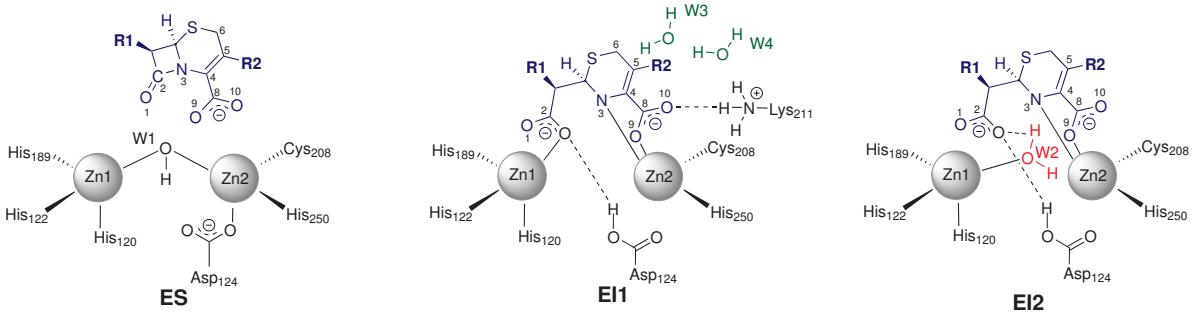

Figure S6: Atom numbers and atom labels as used in Table S4 are shown.

The reaction **EI1** $\rightarrow$ **EI2**, **EI2**$'$ $\rightarrow$ **EI3**$'$ and **EI3**$'$ $\rightarrow$ **EI4**$'$ were modeled using well–sliced metadynamics technique (WS–MTD).[3] In these simulations, umbrella sampling was performed along CV4 while CV5 was treated as metadynamics coordinate (see Table S4). Umbrella windows were having a harmonic force constant of 88 kcal mol^{-1}Å^{-2} placed from 8 Å to 1.5 Å at an interval of 0.005 Å. The initial Gaussian height, hill width and ΔT parameters were 0.6 kcal mol^{-1}, 0.05 and 3000 K, respectively. Langevian thermostat was used for the CV dynamics.

Table S4: Definition of collective coordinates for various elementary steps studied here. The same collective coordinates were used for both the drug molecules. τ indicates metadynamics time.

Reactions	CVs	d^0_{AB} (Å)	p	q	τ (ps)
Path 1 : ES → EI1 → EI2 → EI3 → EP					
ES → EI1	CV1 = C[O_{W1}...(Zn1, Zn2)]	2.75	8	12	25
	CV2 = C[O_{W1}...C_2] − C[C_2...N_3]	1.85	6	8	
EI1 → ES	CV2 = C[O_{W1}...C_2] − C[C_2...N_3]	1.85	6	8	10
	CV3 = C[Zn2...N_3]	2.64	6	6	
EI1 → EI2	CV4 = d[Zn1...O_{W2}]				475
(wsmtd)	CV5 = C[Zn1...(O_1, O_{W1})]	2.64	6	6	
EI2 → EI1	CV5 = C[Zn1...(O_1, O_{W1})]	2.64	6	6	6
	CV6 = C[Zn1...O_{W2}]	2.64	6	6	
EI2 → EI3	CV3 = C[Zn2...N_3]	2.64	6	6	11
	CV7 = C[N_3...(H_{W1}, H_{W2}'s)]	2.11	6	6	
EI3 → EP	CV8 = C[Zn2...Asp124:O_δ's]	2.64	6	6	17
	CV9 = C[Zn2...O_9]	2.64	6	6	
Path 2 : ES → EI1 → EI4					
EI1 → EI4	CV3 = C[Zn2...N_3]	2.64	6	6	12
	CV10 = C[N_3...H_{W1}]	2.11	6	6	
Path 3 : ES → EI1 → EI2′ → EI3′ → EI4′	**→ EP1′ → EP2′**				
EI1 → EI2′	CV11 = C[C_5...(H_{W3}'s, H_{W4}'s, Lys211:H_ζ's)]	1.33	6	6	10
	CV3 = C[Zn2...N_3]	2.64	6	6	
EI2′ → EI1	CV12 = C[C_5...H_{W3}]	1.33	6	6	15
	CV13 = C[Lys211:N_ζ...(H_{W3}'s, H_{W4}'s, Lys211:H_ζ's)]	1.33	6	6	
EI2′ → EI3′	CV4 = d[Zn1...O_{W2}]				380
(WS-MTD)	CV5 = C[Zn1...(O_1, O_{W1})]	2.64	6	6	
EI3′ → EI2′	CV14 = C[Zn2...O_{W2}]	2.64	6	6	8
	CV3 = C[Zn2...N_3]	2.64	6	6	
EI3′ → EI4′	CV4 = d[Zn1...O_{W2}]				190
(WS-MTD)	CV5 = C[Zn1...(O_1, O_{W1})]	2.64	6	6	
EI4′ → EP1′	CV8 = C[Zn2...Asp124:O_δ's]	2.64	6	6	12
	CV9 = C[Zn2...O_9]	2.64	6	6	
EP1′ → EP2′	CV15 = C[O_{W5}...H_{W5}]	1.33	6	6	3
	CV16 = C[O_{W6}...H_{W6}]	1.33	6	6	
Path 4 : ES → EI1 → EI2 → EI3 → EI6′					
EI3 → EI6′	CV17 = C[N_3...H_{W2}] − C[H_{W2}...C_5]	1.33	6	6	7
	CV18 = C[N_5...C_4] − C[C_4...C_5]	1.42	6	6	
Path 5 : ES → EI1 → EI5					
EI1 → EI5	CV3 = C[Zn2...N_3]	2.64	6	6	10
	CV19 = C[N_3...(H_{W3}'s, H_{W4}'s, Lys211:H_ζ's)]	1.33	6	6	

S9 Comparison with Experimental Crystal Structures

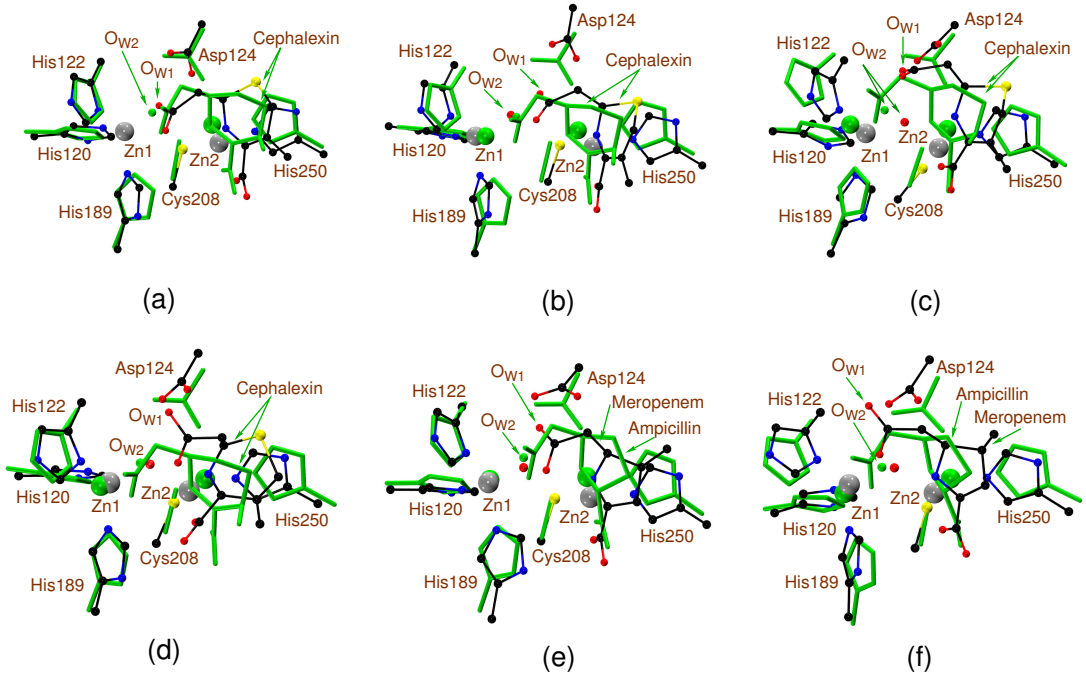

Figure S7: Structural superimposition of the ensemble averaged structure obtained from QM/MM *NVT* simulation of **EI1** (a), **EI2** (b), **EI3** (c) and **EI4′** (d) intermediates (in ball-stick model) of NDM-1:cephalexin with the crystallographic structure (PDB ID: 4RL2;[1] in green color, stick model). Similarly, **EI2** (e) and **EI3** (f) intermediates of NDM-1:meropenem is overlapped with the crystallographic structure (PDB ID: 3Q6X,[4] respectively).

Table S5: Average distances (Å) of various NDM-1:cephalexin reaction intermediates obtained from NVT equilibration.

Distance (Å)		Cephalexin			4RL2[1] (2.0Å)		4RL0[1] (1.3Å)	
	EI1	**EI2**	**EI3**	**EI2′**	Chain A	Chain B	Chain A	Chain B
Zn1...O_{W2}	–	1.95±0.06	1.96±0.05	–	1.8	2.0	2.0	2.0
Zn2...O_{W2}	–	3.85±0.22	1.98±0.05	–	3.0	2.8	2.2	2.2
Zn1...Zn2	5.04±0.23	5.41±0.19	3.44±0.12	4.92±0.20	4.5	4.5	3.8	3.8
Zn2...N_3	2.02±0.06	2.03±0.05	3.52±0.18	2.23±0.10	2.4	2.4	2.4	2.3
Zn2...O_9	2.16±0.09	2.02±0.06	2.06±0.08	2.01±0.06	2.3	2.3	2.2	2.1
Zn1...O_{W1}	2.03±0.08	3.99±0.17	4.26±0.24	2.04±0.07	2.5	2.4	2.8	2.9
Zn2...O_{W1}	3.97±0.19	4.08±0.27	4.90±0.25	4.01±0.19	4.3	4.3	4.2	4.2
N_3...C_4	1.40±0.02	1.39±0.02	1.39±0.02	1.30±0.02	1.3	1.3	1.3	1.3
C_4...C_5	1.36±0.02	1.38±0.02	1.38±0.02	1.51±0.02	1.4	1.4	1.4	1.4
C_4...C_8	1.53±0.03	1.51±0.03	1.52±0.02	1.54±0.02	1.4	1.4	1.4	1.4
Zn2... Asp124:$O_{\delta 2}$	3.65±0.17	5.42±0.48	3.82±0.25	3.78±0.28	2.2	2.2	2.0	2.0

Table S6: Average distances (Å) of various NDM-1:meropenem reaction intermediates obtained from NVT equilibration.

Distance (Å)		Meropenem		4EYL[2] (1.9Å)		4RBS[5] (2.4Å)		3Q6X[4] (1.3Å)	
	EI1	**EI2**	**EI3**	Chain A	Chain B	Chain A	Chain B	Chain A	Chain B
Zn1...O_{W2}	–	1.98±0.06	2.01±0.06	–	–	–	–	2.1	2.0
Zn2...O_{W2}	–	3.32±0.27	2.04±0.06	–	–	–	–	3.0	3.0
Zn1...Zn2	4.79±0.18	4.62±0.23	3.55±0.11	4.0	3.8	4.0	4.0	4.6	4.6
Zn2...N_3	2.01±0.06	2.01±0.05	3.53±0.25	2.2	2.3	2.1	2.1	2.2	2.2
Zn2...O_9	2.13±0.08	2.07±0.07	2.02±0.07	3.0	2.8	2.9	3.1	2.2	2.2
Zn1...O_{W1}	2.07±0.06	3.49±0.27	6.07±0.36	2.2	2.2	1.9	2.1	2.4	2.5
Zn2...O_{W1}	3.76±0.17	4.90±0.20	6.10±0.31	2.4	2.6	3.2	2.9	4.3	4.3
N_3...C_4	1.38±0.02	1.37±0.02	1.38±0.02	1.2	1.3	1.3	1.3	1.5	1.5
C_4...C_5	1.38±0.01	1.39±0.02	1.38±0.02	1.3	1.3	1.3	1.3	1.5	1.5
C_4...C_8	1.50±0.02	1.50±0.02	1.51±0.03	1.3	1.3	1.3	1.3	1.5	1.5
Zn2... Asp124:$O_{\delta 2}$	3.19±0.26	4.70±0.32	4.70±0.21	2.3	2.1	2.2	2.1	2.1	2.1

S10 Committor Analysis

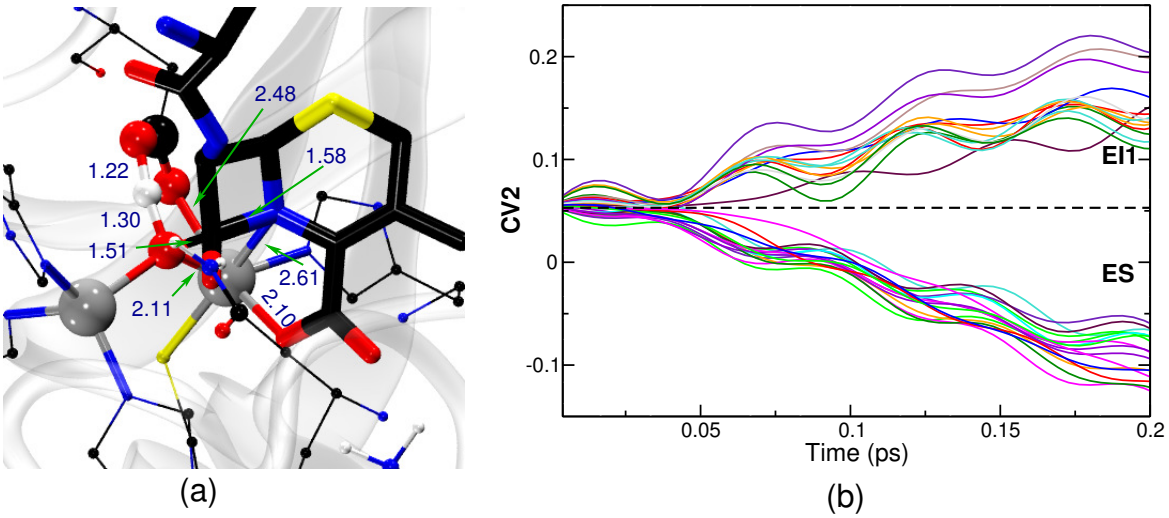

Figure S8: Committor probability is computed here for the transition state structure (see Figure S8(a)) corresponding to **ES** $\rightarrow$ **EI1** for NDM-1:meropenem obtained from metadynamics simulation. Out of the total 30 trajectories that we have lunched, 16 trajectories have proceeded to **ES** and rest of them have proceeded to **EI1** as clear from the plot of CV2 along these trajectories (see Figure S8(b)). The committor probability is therefore close to 50% (53% and 47% exactly).

S11 PBE Error Analysis

To estimate the accuracy of the PBE functional used in our calculation, we had computed the difference between the potential energy barrier for the β–lactam ring–opening step (**ES** $\rightarrow$ **EI1**) using PBE and more reliable MPW1K hybrid functionals. MM part was treated using AMBER Parm99[6] MM force fields. Two layered ONIOM[7] calculations were performed using the Gaussian 09[8] program. QM/MM partitioning remains unchanged in these calculations. 6-31++G(d) basis set was used for the QM part. Single point calculations were performed with the optimized structure for the **ES** and the transition state for the reaction **ES** $\rightarrow$ **EI1** with electronic embedding scheme.

Table S7: Potential energy barrier $\Delta U^{\ddagger}$ (kcal/mol) calculated for QM/MM system with MPW1K and PBE functionals.

Reaction	$\Delta U^{\ddagger}_{\mathrm{MPW1K}}$	$\Delta U^{\ddagger}_{\mathrm{PBE}}$	Error= $\Delta U^{\ddagger}_{\mathrm{MPW1K}}$ - $\Delta U^{\ddagger}_{\mathrm{PBE}}$
ES $\rightarrow$ **EI1**	24.55	23.50	1.05

S12 Free energy surfaces for Cephalexin hydrolysis

S12.1 Path 1

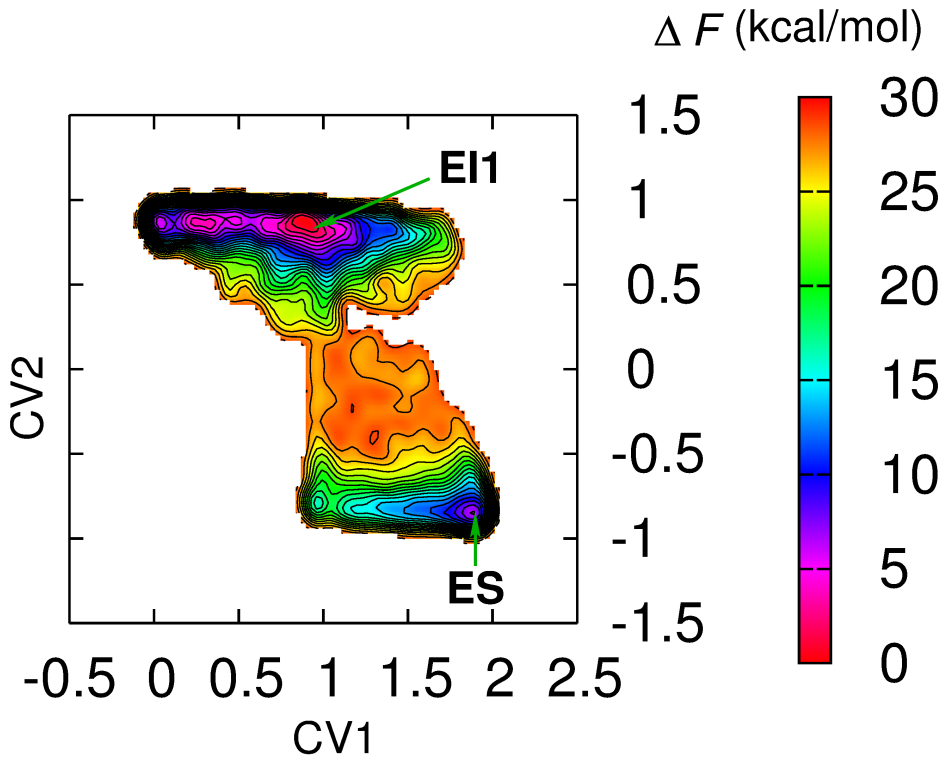

Figure S9: Reconstructed free energy surface for the reaction **ES** → **EI1**

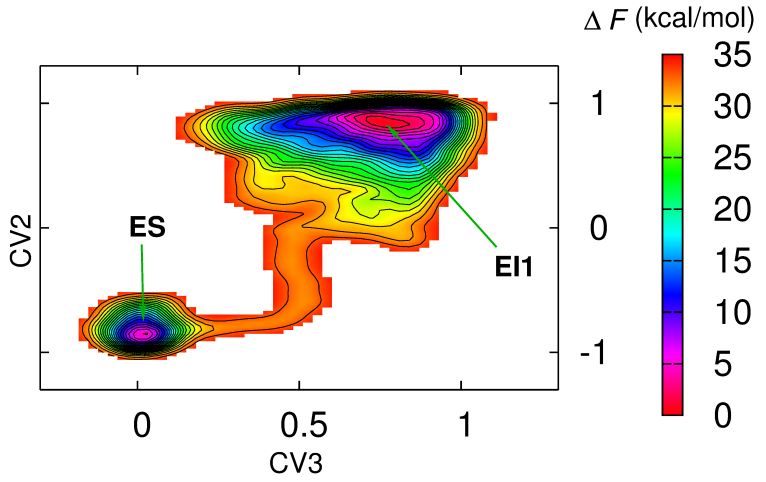

Figure S10: Reconstructed free energy surface for the reaction **EI1** → **ES**

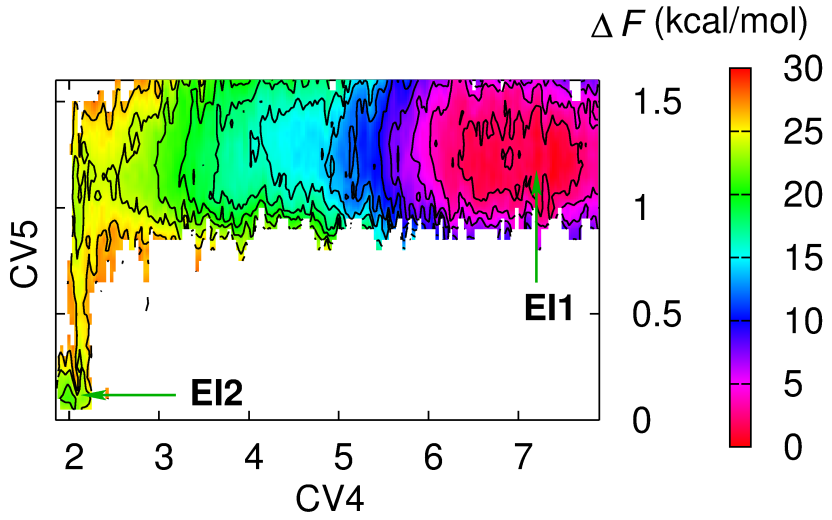

Figure S11: Reconstructed free energy surface for the reaction **EI1** → **EI2**

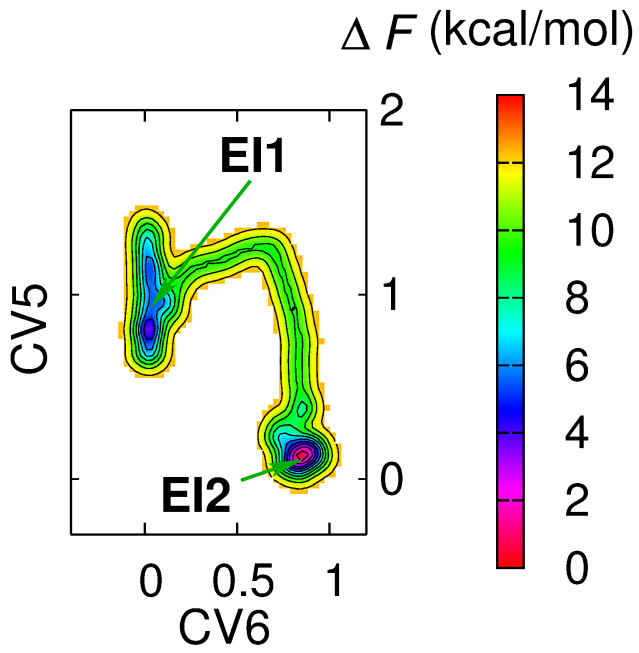

Figure S12: Reconstructed free energy surface for the reaction **EI2** → **EI1**

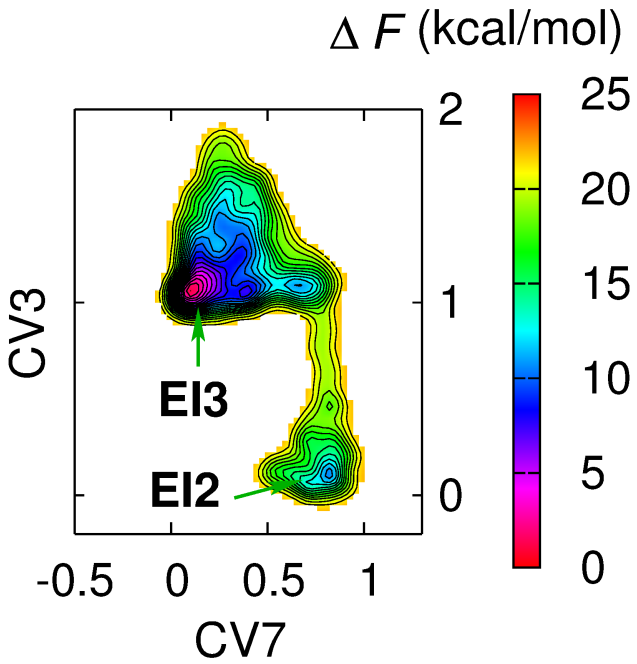

Figure S13: Reconstructed free energy surface for the reaction **EI2** → **EI3**

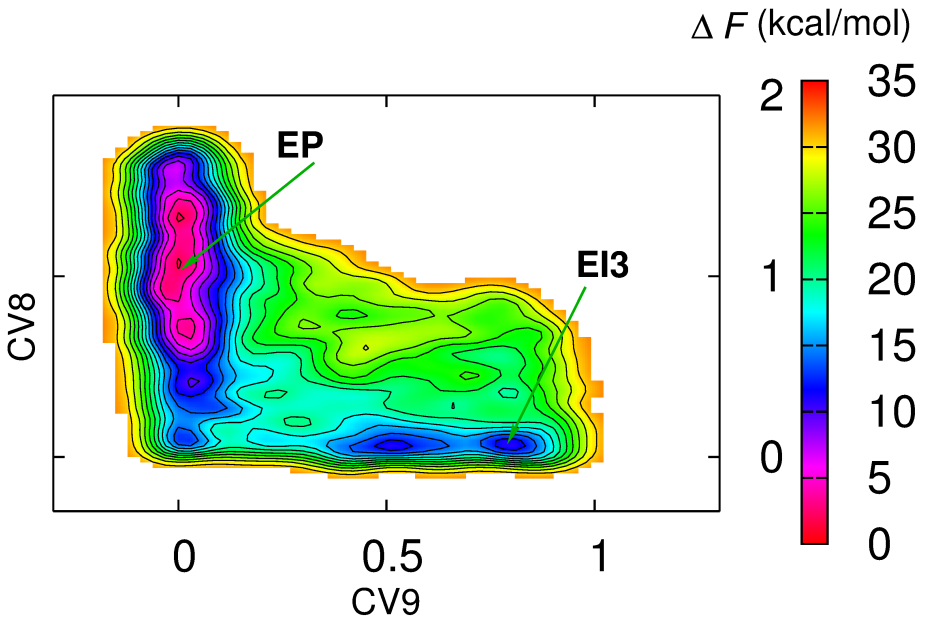

Figure S14: Reconstructed free energy surface for the reaction **EI3** → **EP**

S12.2 Path 2

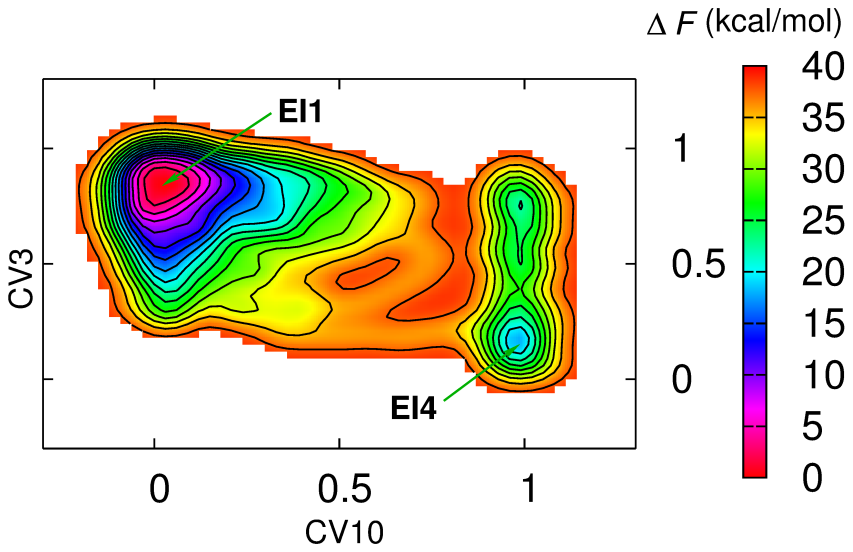

Figure S15: Reconstructed free energy surface for the reaction **EI1** → **EI4**

S12.3 Path 3

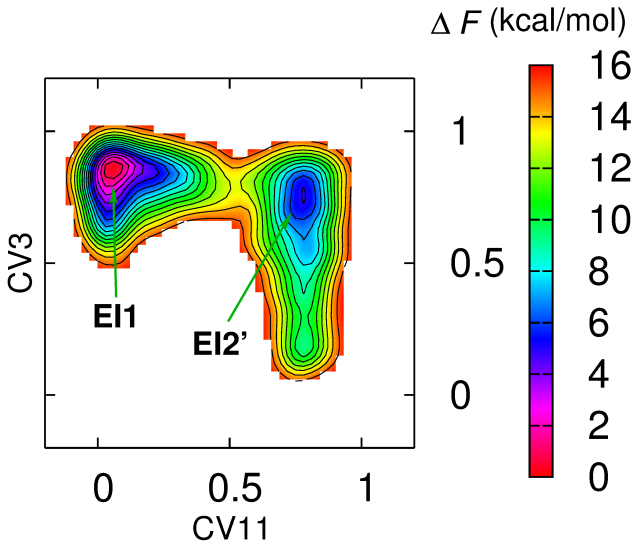

Figure S16: Reconstructed free energy surface for the reaction **EI1** $\rightarrow$ **EI2′**

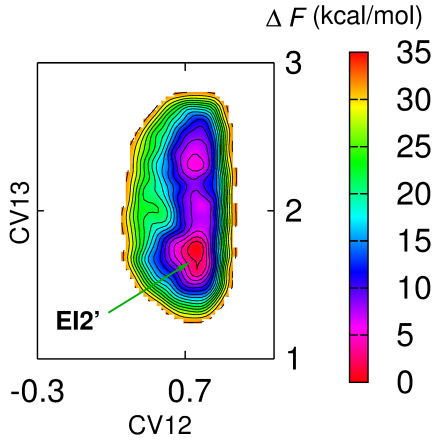

Figure S17: Reconstructed free energy surface for the reaction **EI2′** $\rightarrow$ **EI1**

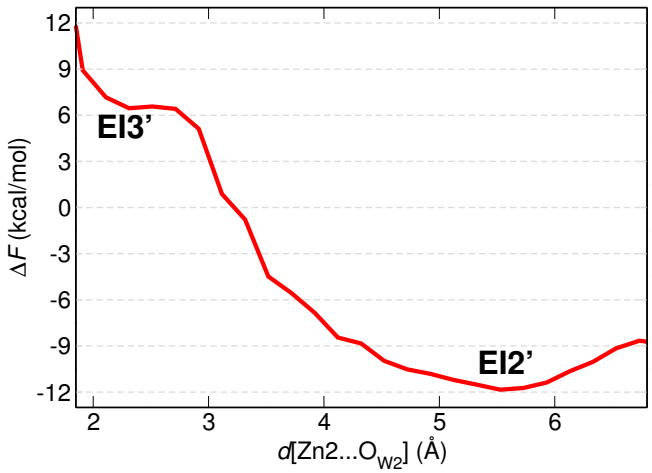

Figure S18: Reconstructed free energy surface for the reaction **EI2′** → **EI3′**

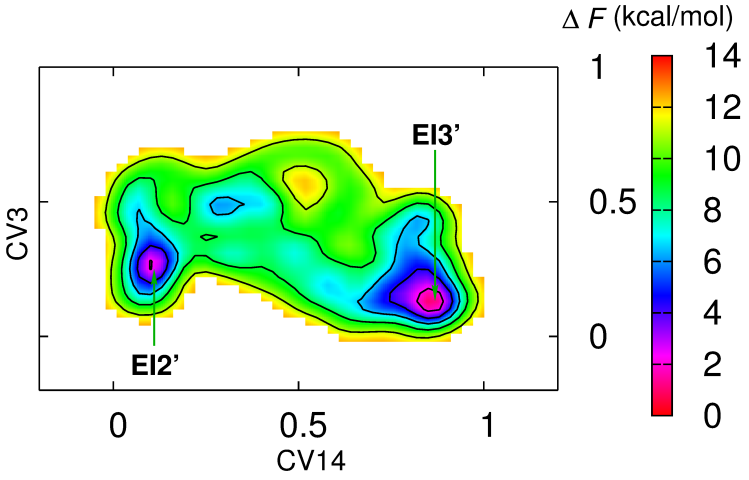

Figure S19: Reconstructed free energy surface for the reaction **EI3′** → **EI2′**

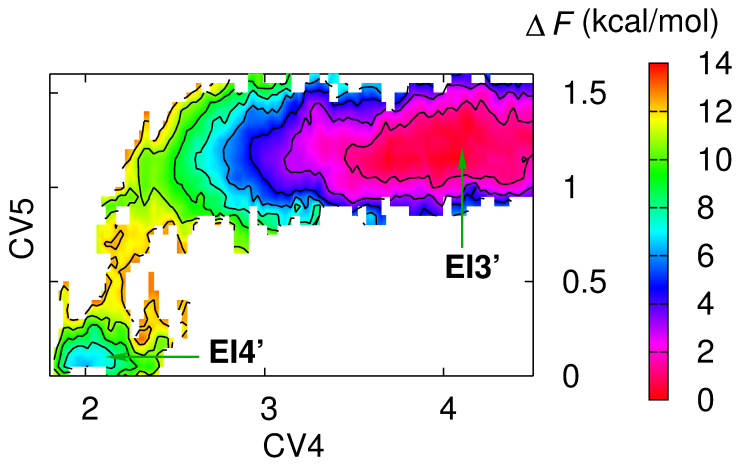

Figure S20: Reconstructed free energy surface for the reaction **EI3′** → **EI4′**

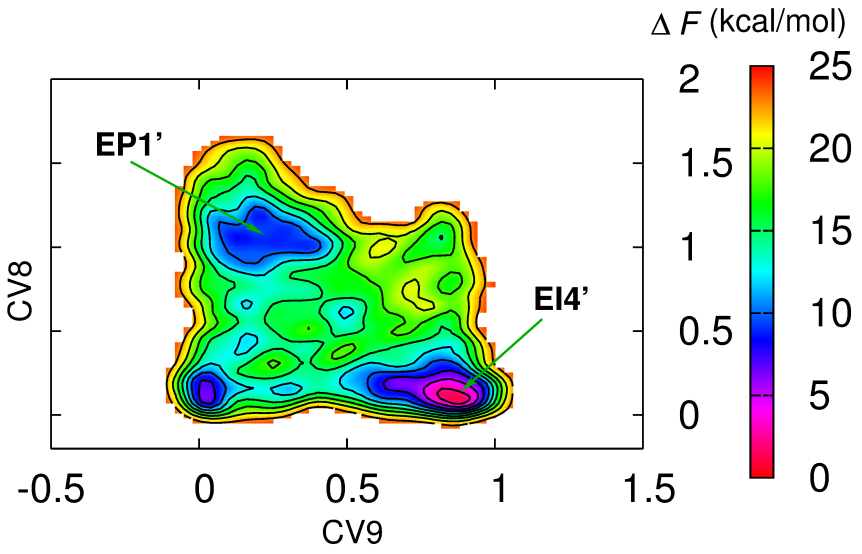

Figure S21: Reconstructed free energy surface for the reaction **EI4′** → **EP1′**

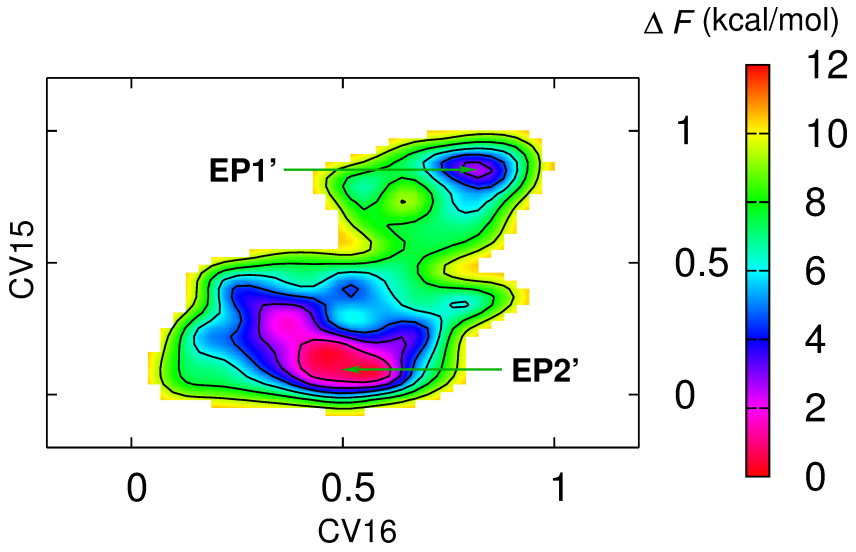

Figure S22: Reconstructed free energy surface for the reaction **EP1**′ → **EP2**′

S12.4 Path 4

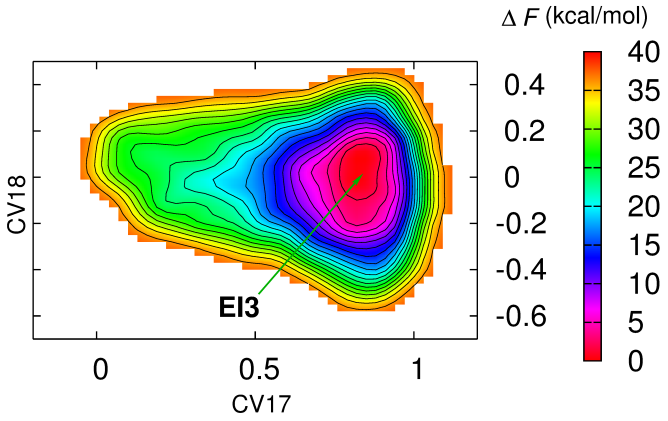

Figure S23: Reconstructed free energy surface for the reaction **EI3** $\rightarrow$ **EI6′**

S12.5 Path 5

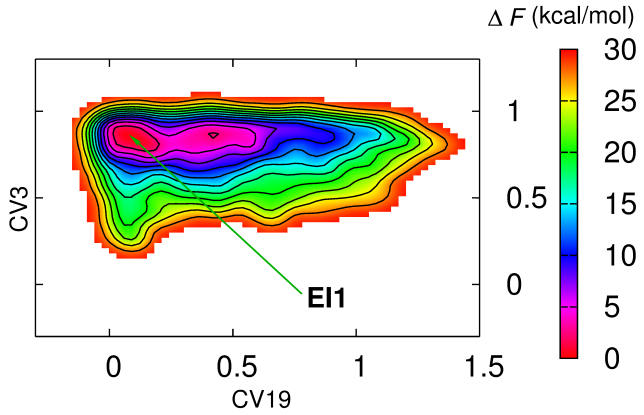

Figure S24: Reconstructed free energy surface for the reaction **EI1** $\rightarrow$ **EI5**

S13 Important Distances of Cephalexin hydrolysis along Path 1 and Path 3

S13.1 Path 1

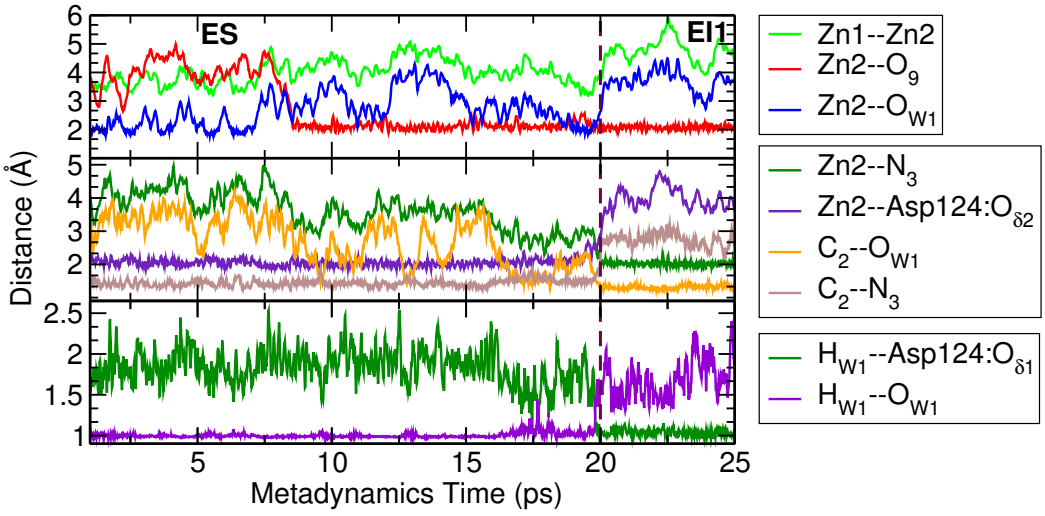

Figure S25: Plots of crucial distances during the reaction of **ES** → **EI1** (**Path 1**).

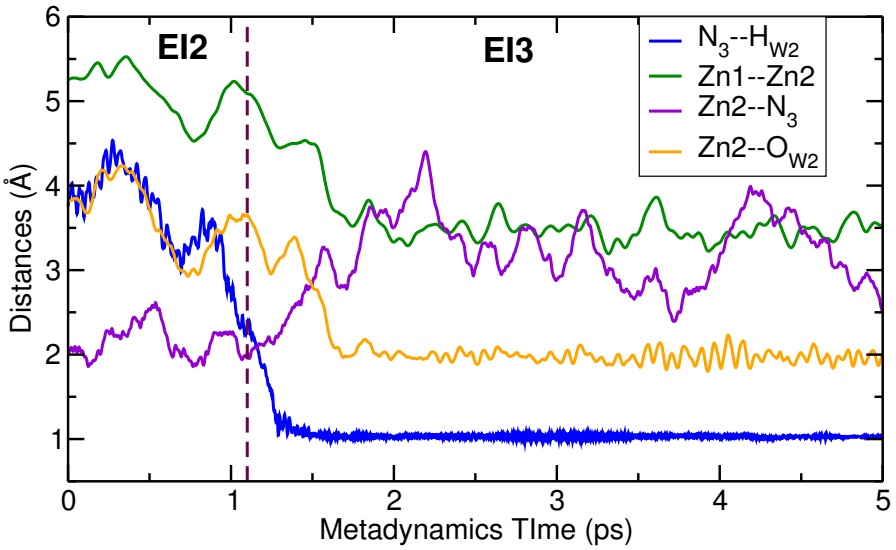

Figure S26: Plots of crucial distances during the reaction of **EI2** → **EI3** (**Path 1**).

S13.2 Path 3

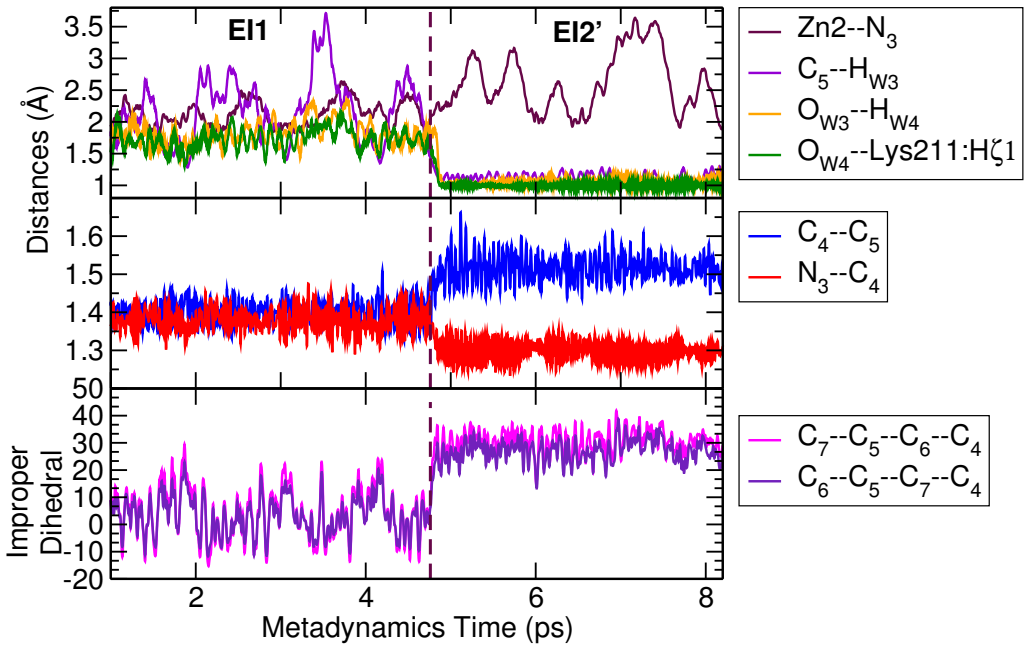

Figure S27: Plots of crucial distances and improper dihedral angles during the reaction of **EI1** $\rightarrow$ **EI2′** (**Path 3**).

S14 Free Energy Surfaces for Meropenem Hydrolysis by NDM-1 along Path 1

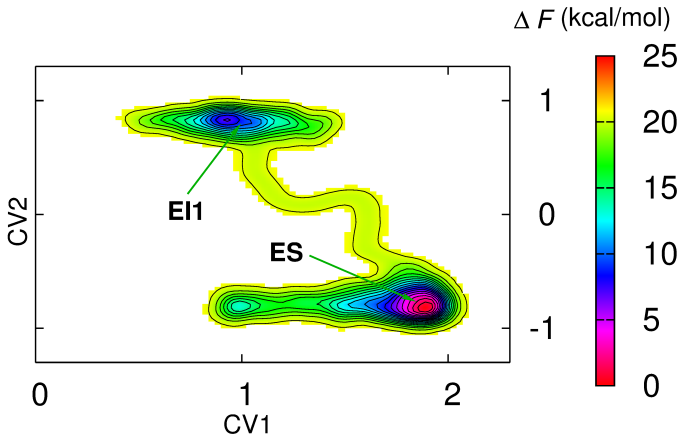

Figure S28: Reconstructed free energy surface for the reaction **ES** → **EI1**

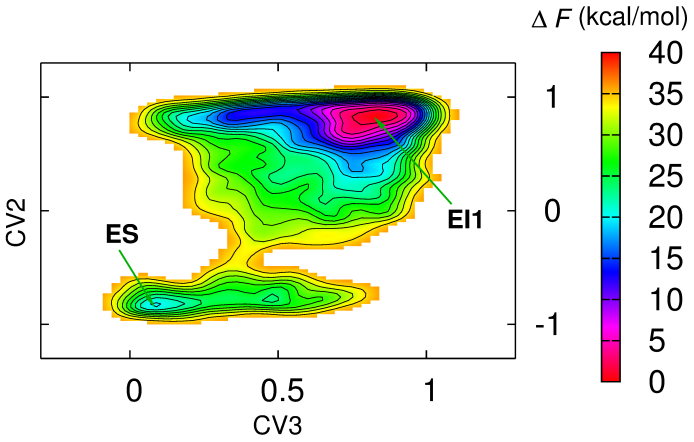

Figure S29: Reconstructed free energy surface for the reaction **EI1** → **ES**

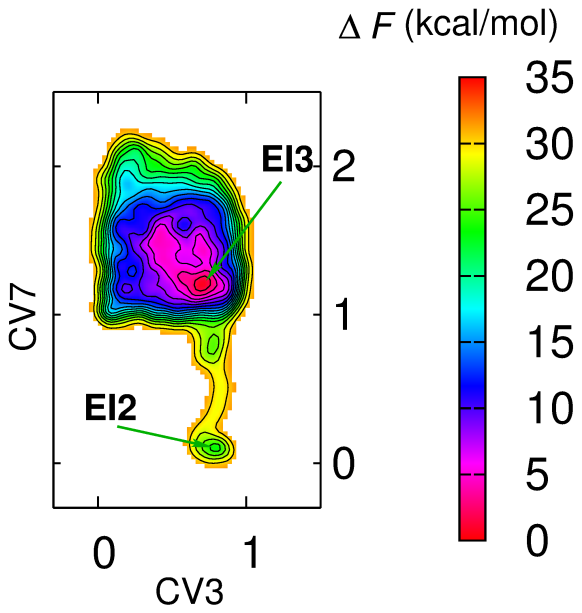

Figure S30: Reconstructed free energy surface for the reaction **EI2** → **EI3**

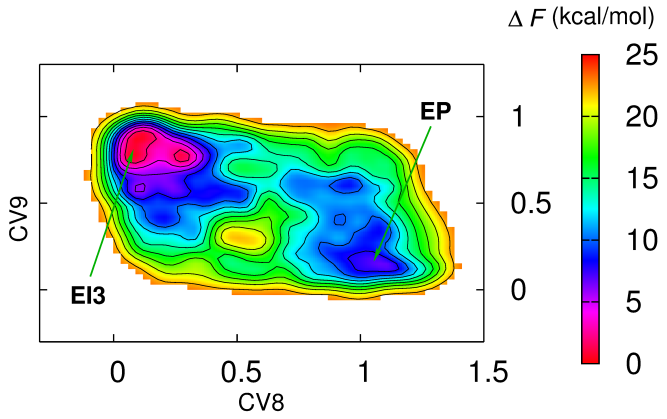

Figure S31: Reconstructed free energy surface for the reaction **EI3** → **EP**

References

(1) H. Feng, J. Ding, D. Zhu, X. Liu, X. Xu, Y. Zhang, S. Zang, D. Wang and W. Liu, *J. Am. Chem. Soc.*, 2014, **136**, 14694–14697.

(2) D. T. King, L. J. Worrall, R. Gruninger and N. C. J. Strynadka, *J. Am. Chem. Soc.*, 2012, **134**, 11362–11365.

(3) S. Awasthi, V. Kapil and N. N. Nair, *J. Comp. Chem.*, 2016, **37**, 1413–1424.

(4) H. Zhang and Q. Hao, *FASEB J.*, 2011, **25**, 2574–2582.

(5) T. C. Kim, Y., R. Jedrzejczak, J. Babnigg, G.and Sacchettini and A. Joachimiak.

(6) T. E. Cheatham, P. Cieplak and P. A. Kollman, *J. Biomol. Struct. Dyn.*, 1999, **16**, 845–862.

(7) S. Dapprich, I. Komáromi, K. S. Byun, K. Morokuma and M. J. Frisch, *J. Mol. Struct. (Theochem)*, 1999, **461-462**, 1–21.

(8) M. J. Frisch, G. W. Trucks, H. B. Schlegel, G. E. Scuseria, M. A. Robb, J. R. Cheeseman, G. Scalmani, V. Barone, B. Mennucci, G. A. Petersson, H. Nakatsuji, M. Caricato, X. Li, H. P. Hratchian, A. F. Izmaylov, J. Bloino, G. Zheng, J. L. Sonnenberg, M. Hada, M. Ehara, K. Toyota, R. Fukuda, J. Hasegawa, M. Ishida, T. Nakajima, Y. Honda, O. Kitao, H. Nakai, T. Vreven, J. J. A. Montgomery, J. E. Peralta, F. Ogliaro, M. Bearpark, J. J. Heyd, E. Brothers, K. N. Kudin, V. N. Staroverov, T. Keith, R. Kobayashi, J. Normand, K. Raghavachari, A. Rendell, J. C. Burant, S. S. Iyengar, J. Tomasi, M. Cossi, N. Rega, J. M. Millam, M. Klene, J. E. Knox, J. B. Cross, V. Bakken, C. Adamo, J. Jaramillo, R. Gomperts, R. E. Stratmann, O. Yazyev, A. J. Austin, R. Cammi, C. Pomelli, J. W. Ochterski, R. L. Martin, K. Morokuma, V. G. Zakrzewski, G. A. Voth, P. Salvador, J. J. Dannenberg, S. Dapprich, A. D. Daniels, O. Farkas, J. B. Fores-

man, J. V. Ortiz, J. Cioslowski and D. J. Fox., *Gaussian 09, Revision B.01*, Gaussian, Inc., Wallingford CT, 2010.